Accepted Manuscript

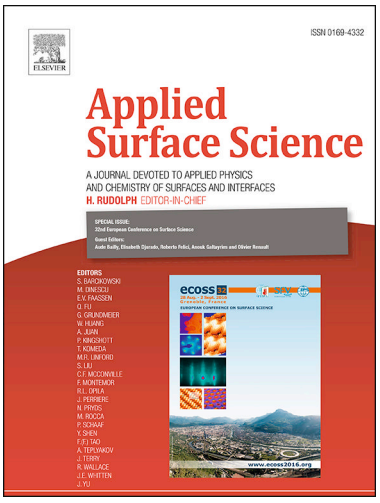

Full Length Article

The Effect of Aluminium Nanocoating and Water pH Value on The Wettability Behavior of an Aluminium Surface

Naser Ali, Joao A. Teixeira, Abdulmajid Addali, Feras Al-Zubi, Ehab Shaban, Ismail Behbehani

PII: S0169-4332(18)30537-3
DOI: https://doi.org/10.1016/j.apsusc.2018.02.182
Reference: APSUSC 38640

To appear in: *Applied Surface Science*

Received Date: 17 August 2017
Revised Date: 15 January 2018
Accepted Date: 18 February 2018

Please cite this article as: N. Ali, J.A. Teixeira, A. Addali, F. Al-Zubi, E. Shaban, I. Behbehani, The Effect of Aluminium Nanocoating and Water pH Value on The Wettability Behavior of an Aluminium Surface, *Applied Surface Science* (2018), doi: https://doi.org/10.1016/j.apsusc.2018.02.182

Applied Surface Science, Volume 443, 15 June 2018, Pages 24-30
DOI: 10.1016/j.apsusc.2018.02.182

The Effect of Aluminium Nanocoating and Water pH Value on The Wettability Behavior of an Aluminium Surface

Naser Ali[*1,2,a], Joao A. Teixeira[1,b], Abdulmajid Addali [1,c], Feras Al-Zubi [2,d], Ehab Shaban [2,e], and Ismail Behbehani [3,f]

[1]*Cranfield University, School of Water, Energy and Environment (SWEE), Cranfield, England, MK430AL, UK*
E-mail: naser.ali@cranfield.ac.uk, j.a.amaral.teixeira@cranfield.ac.uk, a.addali@cranfield.ac.uk

[2]*Nanotechnology and Advanced Materials Program, Energy and Building Research Center, Kuwait Institute for Scientific Research, Safat 13109, Kuwait*
E-mail: nmali@kisr.edu.kw, fzubi@kisr.edu.kw, ehabshaban@gmail.com

[3]*Ministry of Public Works, Materials Department, Safat 13001, Kuwait*
E-mail: ibhbhani@gmail.com

*Corresponding Author (nmali@kisr.edu.kw)

The Effect of Aluminium Nanocoating and Water pH Value on The Wettability Behavior of an Aluminium Surface

Naser Ali[*1,2,a], Joao A. Teixeira[1,b], Abdulmajid Addali [1,c], Feras Al-Zubi [2,d], Ehab Shaban [2,e], and Ismail Behbehani [3,d]

[1]*Cranfield University, School of Water, Energy and Environment (SWEE), Cranfield, England, MK430AL, UK*

E-mail: naser.ali@cranfield.ac.uk, j.a.amaral.teixeira@cranfield.ac.uk, a.addali@cranfield.ac.uk

[2]*Nanotechnology and Advanced Materials Program, Energy and Building Research Center, Kuwait Institute for Scientific Research, Safat 13109, Kuwait*

E-mail: nmali@kisr.edu.kw, fzubi@kisr.edu.kw, ehabshaban@gmail.com

[3]*Ministry of Public Works, Materials Department, Safat 13001, Kuwait*

E-mail: ibhbhani@gmail.com

*Corresponding Author (nmali@kisr.edu.kw)

A B S T R A C T

Experimental investigation was performed to highlight the influence of ionic bounding and surface roughness effects on the surface wettability. Nanocoating technique via e-beam physical vapour deposition process was used to fabricate aluminium (Al) film of 50, 100, and 150 nm on the surface of an Al substrate. Microstructures of the samples before and after deposition were observed using an atomic force microscopy. A goniometer device was later on used to examine the influence of surface topography on deionised water of pH 4, 7 and 9 droplets at a temperature ranging from 10°C to 60°C through their contact angles with the substrate surface, for both coated and uncoated samples. It was found that, although the

coated layer has reduced the mean surface roughness of the sample from 10.7 nm to 4.23 nm, by filling part of the microstructure gaps with Al nanoparticles, the wettability is believed to be effected by the ionic bounds between the surface and the free anions in the fluid. As the deionised water of pH 4, and 9 gave an increase in the average contact angles with the increase of the coated layer thickness. On the other hand, the deionised water of pH 7 has showed a negative relation with the film thickness, where the contact angle reduced as the thickness of the coated layer was increased. The results from the aforementioned approach had showed that nanocoating can endorse the hydrophobicity (unwitting) nature of the surface when associated with free ions hosted by the liquid.

Keywords: Hydrophobic; hydrophilic; surface topography; element analysis; coating; contact angle.

1. **Introduction**

Nanoparticles have gained wide recognition in a variety of industrial and commercial applications over the years, such as sunscreen products [1] , medicine [2, 3], electronics [4], transportation [5], reduction of buildings pollution [6], magnetic sealing [7], microbial fuel cells [8], space and defence [9], and structural applications [10].

Alumina (Al_2O_3), in specific, possesses a variety of industrial and commercial uses and has become one of the important elements that is used in manufacturing commercial ceramic materials [11, 12]. On the nano scale, nanoparticles of Al_2O_3 have been used to produce nanocomposites [13, 14], polymer modification [15], textiles functionalization [16], wastewater treatment [17], heat transfer fluids [18], surface coating [19], and as catalysis [20-22].

Surface friction and wettability are important in many of these applications, however, they require further advancement. Whereas in piping systems, the inner pipe surface friction plays a prominent role in the determination of the pressure drop through the head losses along the pipelines for flows of turbulent state. This is theoretically proven using the non-linear relationship between the Reynold number (Re) and the implicit Colebrook–White equation [23], which are expressed in form of a formulation as,

$$Re = \frac{V.D}{\upsilon} \quad (1)$$

$$\frac{1}{\sqrt{f}} = 1.14 - 2\,log_{10}\left(\frac{\varepsilon/D}{3.7} + \frac{2.523}{Re\sqrt{f}}\right) \quad (2)$$

Where υ, D, V, f, and ε are kinematic viscosity, inner pipe diameter, inner pipe average flow velocity, Darcy-Welsbach friction factor, and roughness height, respectively.

On the other hand, surface wettability is determined by the angle of contact between a liquid droplet and the surface in contact to it [24]. Where the surface is called "super-hydrophilic" if the angle is less than 5^o, "hydrophilic" if the angle is between 5^o and 90^o, "hydrophobic" if the angle is between 90^o and 150^o, and "super-hydrophobic" if the angle is greater than 150^o [24, 25]. The term hydrophilic reflects the tendency of the fluid to form a strong bond with the surface, where the term hydrophobic indicates the propensity of the fluid to repel from the surface. Once a liquid of an ionic nature, such as water, comes in contact with an aluminium (Al) surface, an ionic reaction occurs in any of the following forms [26, 27].

$$Al + 3H_2O \rightarrow Al(OH)^3 + 3H^+ + 3e^- \quad (1)$$

$$Al + 3/2H_2O \rightarrow Al_2O_3 + 3H^+ + 3e^- \quad (2)$$

$$Al + 2H_2O \rightarrow AlO(OH) + 3H^+ + 3e^- \quad (3)$$

Such reaction leads to a reduction of oxygen (O_2) atoms and production of hydroxyl ions (H^+) and hence changes the hydrophobicity/hydrophilicity nature of the surface [19].

Fluid-solid interaction has its own importance in a range of applications such as designing of water repelling surfaces [28] to fluid flow manipulation in piping systems [24] and inhabitation of machinery corrosion [29].

Kang et al. [24] studied in their work the effect of surface nanocoating on the reduction of liquid pumping power by modifying the contact angle (CA) of the riser surface. The CA's examined were between 23.7° and 153.8° with the highest pumping power efficiency obtained at a CA of 90.3° for the silicon dioxide (SiO_2) coating of concentration 6.67×10^{-3} wt%.

Zhang et al. [30] considered the improvement of heat exchanger, which consist of fins and tubes, thermal performance by depositing titanium dioxide (TiO_2) film on an Al substrate. Baking temperatures of 150°C, 250°C, 350°C, 450°C, and 600°C were implemented using an electric muffle furnace for surface treatment. For the same Re and relative air humidity (RH) condition, the heat transfer coefficient was found to be the highest after baking the coated

substrate at a temperature of 250°C. But decreased when the baking temperature increased above 250°C due to the reduction in coated film area.

Phan et al. [31] investigated experimentally, using nanocoating techniques, the surface wettability effect on nucleate boiling heat transfer. Water CA on a stainless steel grad 301 substrates was varied from 22° to 112° by depositing different coating materials. They found that greater surface wettability decreased the bubble emission frequency but raised the vapor bubble departure radius. Moreover, lower superheat temperature was required to generate the bubbles growth on a hydrophobic surfaces. They also noticed the tendency of bubbles to merge together forming a vapor blanket on the hydrophobic surface leading to critical heat flux (CHF).

Akbari et al. [32] studied the enhancement of saturated pool boiling of distilled water under atmosphere pressure where they formed a layer of silver nanoparticles on a copper substrate by boiling silver nanofluid of 0.025 and 0.05 vol%. They found that higher particles concentration increased the clustering deposition and surface hydrophobicity, however stability of the deposition was reduced. Their results also showed that, the heat transfer coefficient (HTC) and CHF improved by reaching a nanocoated polished surface state.

In this study, the CA and surface roughness of an Al substrate were modified through electron beam physical vapor deposition (e-beam PVD) coating technique to enhance the ionic interaction between the surface and the water droplet. An atomic force microscopy (AFM) device was used to measure the reduction in surface roughness after coating the substrate with 50, 100, and 150 nm thick layers. Furthermore, a goniometer devices was used in an attempt to understanding the influence of free ions imbedded in the liquid on the attached surface CA.

2. **Experimental**

2.1 Materials

All chemicals were used as-received without further purification. Hydrochloric acid (HCl ~37%) grad ACS reagent and acetone ($CH_3\ COCH_3\ \geq 99.5\%$) grad ACS reagent were purchased from SIGMA-ALDRICH, and sodium hydroxide pellets (NaOH ~98%) grad AR was purchased from LOBA Chemie. Al pellets, 3.175 mm diameter and 6.35 mm height, of 99.99% purity was purchased from Kurt J. Lesker Co. Four cylindrical shaped, 25 mm

diameter and 15 mm height, substrates of 92.5% Al were manufactured using a computer numerical control (CNC) machine.

2.2 Preparation of aluminium coatings

Aluminium pellets were placed in a 8 cm^3 graphite crucible to be used as the coating material source and the Al substrate was cleaned by a Soniclean company digital benchtop ultrasonic cleaner filled with acetone for 20 min after which it was wiped carefully before tightly adjusted to the sample holder and positioned vertically inside the e-beam PVD device. The e-beam PVD device chamber was then vacuumed to a pressure of 346.64 x 10^{-6} pa to insure the removal of all particle contaminations within it and to control the level of evaporation. The Al pellets were later on partially evaporated from the crucible and the Al vapor deposited on the substrate surface with a deposition rate of 0.1 Å/s to form a 50, 100, and 150 nm thick layers. After the particle deposition process completion, the substrate was left in the chamber for 4 h to cool down before removal. The coating procedure used for the preparation of the Al layer on the substrate is shown in Fig. 1.

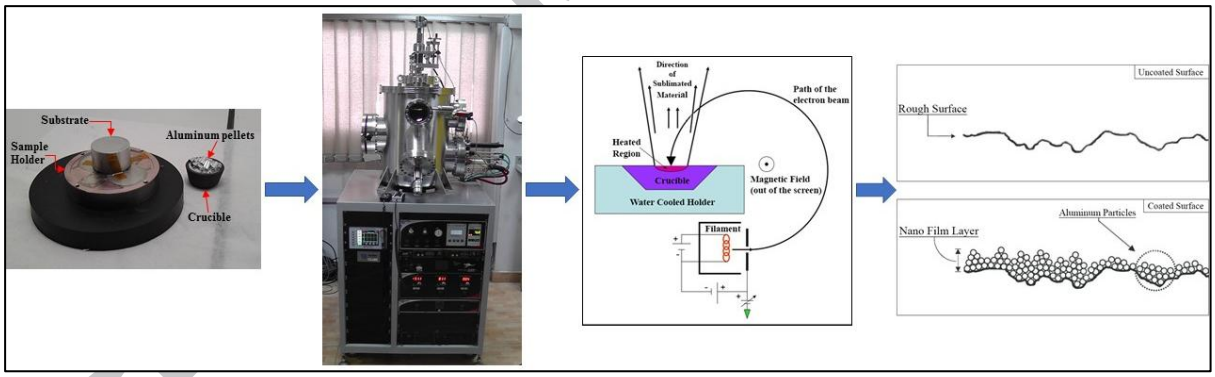

Fig. 1. Aluminium particle deposition procedure.

2.3 Characterization

Elemental analysis of the Al substrates was performed three times and averaged using a BRUKER TITAN S1 x-ray fluorescent (XRF) handheld analyser to insure that the bulk components in the manufactured substrate were of Al base. This was done by placing the substrate on the working station and adjusting the XRF device lens vertically on the substrate before starting the measurements which required 10 seconds to complete for each measurement. Additional elemental test was performed through a 9 kW Rigaku SmartLab, Japan, x-ray diffraction (XRD) analyser and its software, SmartLab Guidance, using a CuKα X-ray source with a diffraction angle of 2Θ and an incidence beam angle of 0.02° to

determine the Bragg's peaks of each element contained in the substrate. The diffraction scanning angle ranges were from 20° to 80° at a scanning rate of 2°/min. A Keysight Technologies 5600LS AFM in tapping mode was used to illustrate the changes in surface topography of the coated and uncoated substrates. The particles size of Al_2O_3 film and surface roughness were determined using Mountview software. Surface wettability was measured by preparing three beakers of 250 ml that were filled with 150 ml of deionised water (DIW) of pH 7 in each. Two of the three DIW, contained in the beakers, pH levels were adjusted to 4 by adding HCl and 9 by adding NaOH. The pH level in each beaker was measured using a HACH HQ11D portable pH meter with accuracy of 0.002 pH. The samples were then used separately to fill one of three 500 µl glass syringes, purchased from Hamilton company, each time. The three syringes containing DIW of pH 4, 7, and 9 were then placed on the Dataphysics OCA 100 contact angle goniometer device automatic multi liquid dispenser. The surface wettability was then measured at a liquid temperature of 10, 20, 25, 30, 40, 50, and 60°C, by heating/cooling the fluid sample using a Dataphysics SHD syringe temperature controller, for the coated and uncoated substrates through the determination of liquid/surface CA using the device supplied software, SCA 20. For each test, the volume of 3 µl liquid drop was carefully dropped on the surface of the test samples with a dosing rate of 3 µl/s and under ambient conditions. The average angle value for each sample was later on reported with a precision value of ± 0.1°. The image of the drop was captured by a high speed video camera provided with the device.

3. **Results and discussion**

3.1 X-ray fluorescent (XRF) and x-ray diffraction (XRD) analysis

The elemental content of the substrates manufactured, as examined by the XRF for three times and averaged, are given in Table 1. In addition to the XRF results, the XRD pattern showed good agreement with the XRF analysis as suggested by the sharp diffraction Bragg's peaks (PDF Card No.: 01-089-2837) shown in Fig. 2. This conforms that the bulk formation of the substrate is of Al base.

Table 1. Averaged XRF elemental analysis of the aluminium substrate.

Element	Percentage			
	Minimum	Maximum	Content	(+/-) Error
Aluminium	90	96	92.5	0.04
Iron	0	0.7	0.56	0.03
Copper	5	6	5.82	0.06
Zinc	0	0.3	0.05	0.01
Lead	0.2	0.6	0.43	0.02

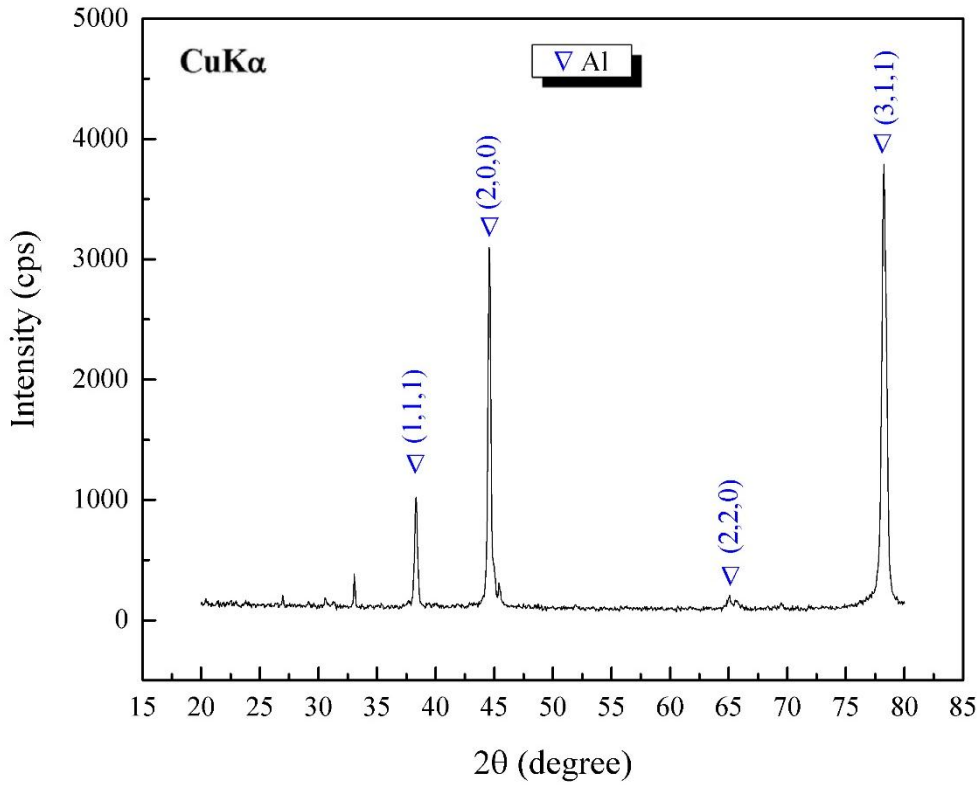

Fig. 2. X-ray diffraction pattern of Al substrate.

3.2 Surface characterization

Fig. 3 represents the topographical two and three dimensional images obtained from the AFM device for the coated and uncoated samples. The 3D profile shown in Fig. 3(B, D, F, and H) clearly reveals the reduction in surface roughness of the substrate caused from the increase in Al film thickness in comparison to the uncoated substrate shown in Fig. 3(B). This is because

the surface roughness depends on the height variation on the surface which can be classified into micro gaps, hills, and valleys [33].

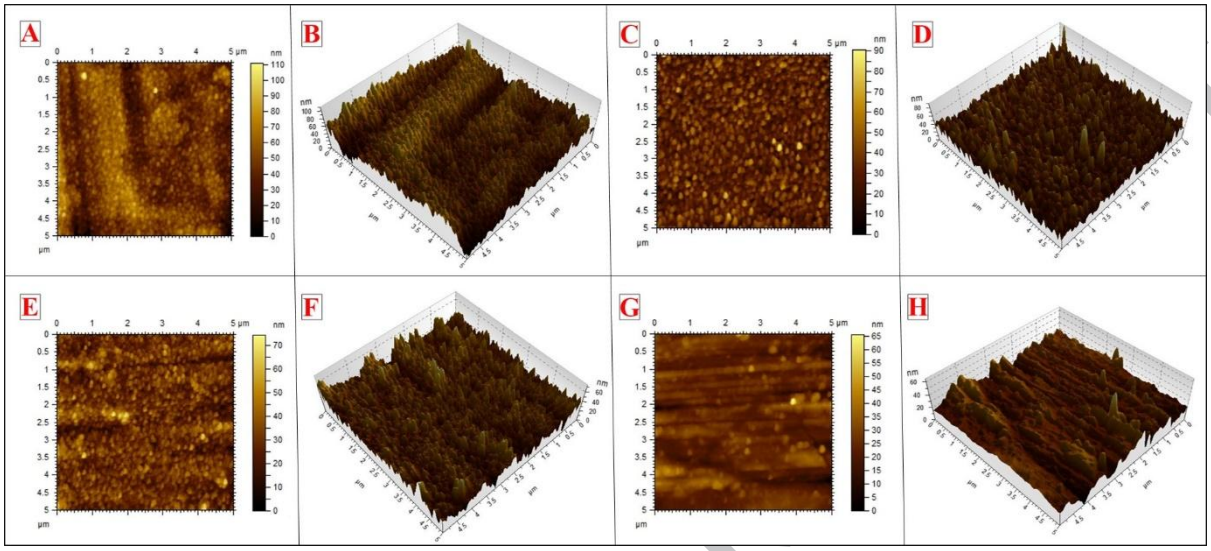

Fig. 3. Atomic force microscopy images of: (A) 2D profile of uncoated sample, (B) 3D profile of uncoated sample, (C) 2D profile of 50 nm coated sample, (D) 3D profile of 50 nm coated sample, (E) 2D profile of 100 nm coated sample, (F) 3D profile of 100 nm coated sample, (G) 2D profile of 150 nm coated sample, and (H) 3D profile of 150 nm coated sample.

In the case of the uncoated sample, the hills are found to be high which implies that the surface is of greater surface roughness. This is because the nanostructures on the surface have a range of height between 33.3 to 99.8 nm and a root mean square height (RMSH) of 13.4 nm which shows a wide variety of disparity as seen in Fig. 4(A). On the other hand, the coated samples exhibited less hills and valleys with minimum micro gaps, as the film thickness increases, compared to the uncoated sample. This can be attributed to the sealing of the micro gaps as a result of the deposition of Al particles on the surface, where at a coated thickness of 150 nm, about 95% of the nanostructures on the surface have height between 32.8 and 52.4 nm with the maximum height found to be 59 nm as illustrated in Fig. 4(D) and a RMSH value of 5.56 nm. This clear difference in height distribution and values is an indication of rougher surface of the uncoated sample which was smoothened out by the deposition of nanofilm deposited on the surface. As the mean surface roughness values were found to be 10.7, 7.51, 6.32, and 4.23 nm for the uncoated, 50 nm, 100nm, and 150 nm coated substrates, respectively as shown in Fig. 4(A-D).

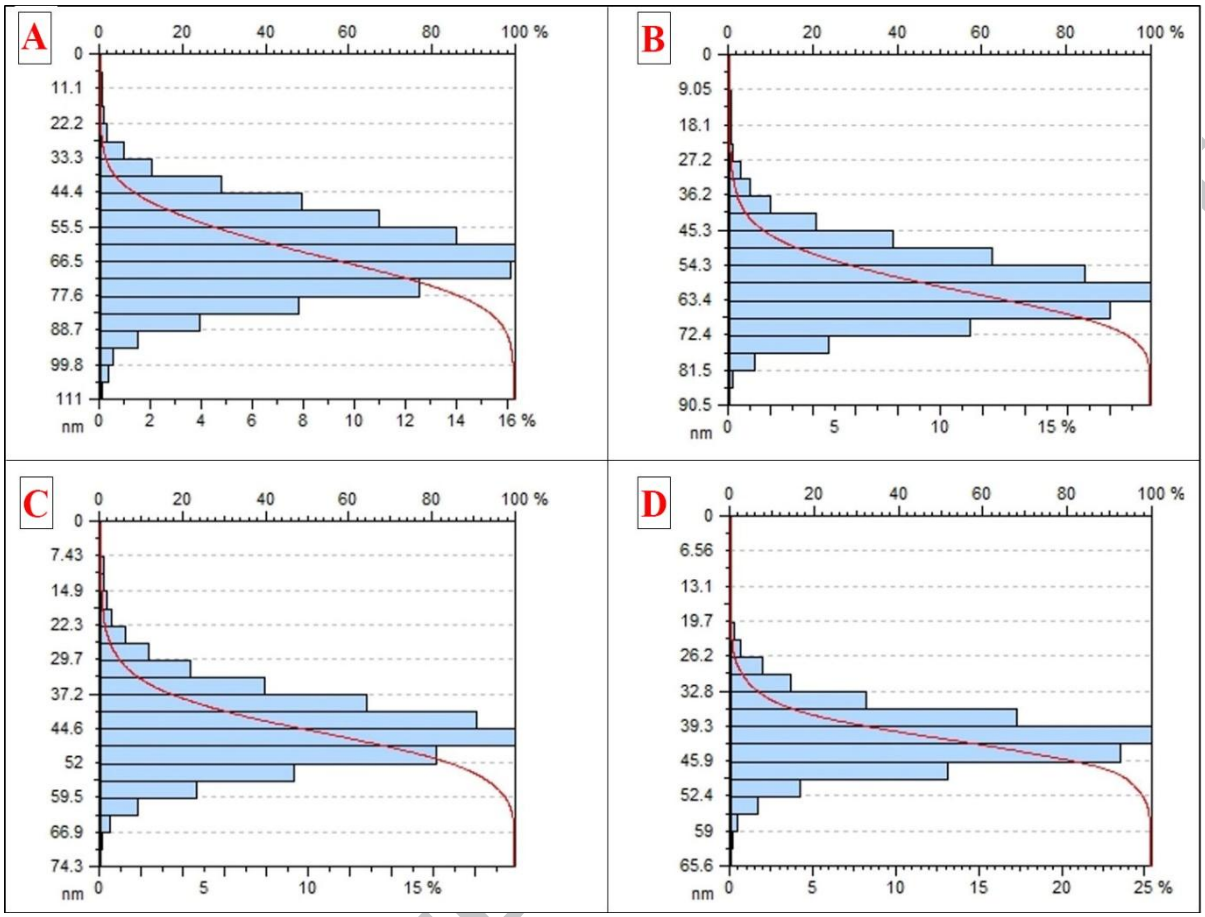

Fig. 4. Particles height distribution of: (A) Uncoated substrate surface, (B) 50 nm coated substrate surface, (C) 100 nm coated substrate surface, and (D) 150 nm coated substrate surface.

3.3 Water contact angle (CA) measurement

The surface wettability of the Al substrates, both coated and uncoated, were examined via liquid/surface CA measurements at different liquid temperatures and film thickness with the results demonstrated in Fig. 5. In the case where DIW of pH 7 was used as the testing fluid, the CA of the uncoated sample showed a higher average value than the coated samples in all cases. This suggest that the surface wettability nature was changed to a higher hydrophilic surface caused from the deposited particles and the neutral charged liquid. The minimum CA was recorded at a temperature of 25°C with a value of 55.3°, as demonstrated in Fig. 5(C). On the other hand, when tested the samples with DIW of pH 4 and 9, the hydrophilicity nature of the surface diverged more towards the hydrophobicity region, and in some cases, achieving a fully hydrophobic surface nature as seen in Fig. 5(A-G). The maximum increase

in CA was obtained at a temperature of 60°C, a pH of 9, and a film thickness of 150 nm where the CA raised from 71° to 100.1° as illustrated in Fig. 5(G).

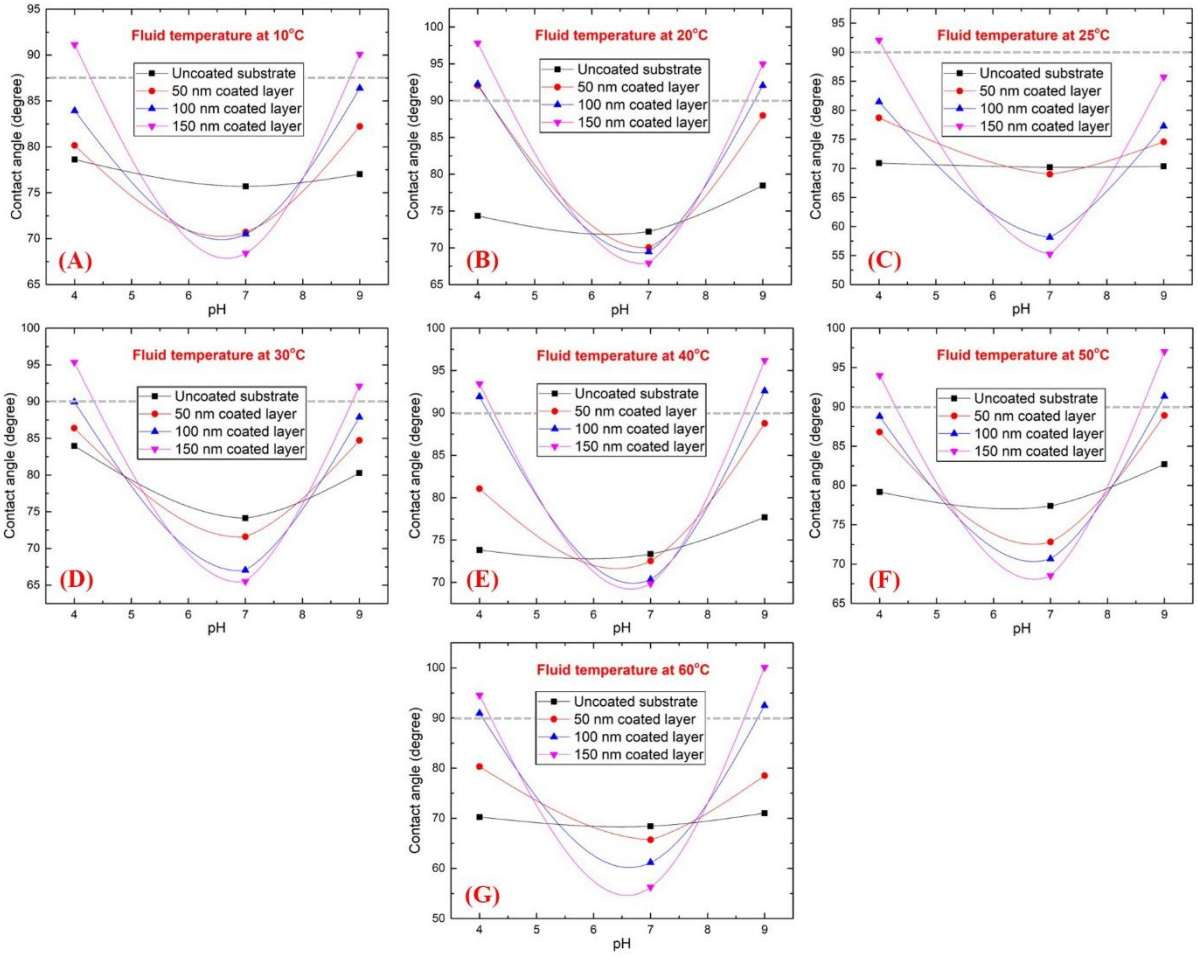

Fig. 5. Contact angle measurements of coated and uncoated Al substrates with DIW of pH 4, 7, and 9 at: (A) 10°C fluid temperature, (B) 20°C fluid temperature, (C) 25°C fluid temperature, (D) 30°C fluid temperature, (E) 40°C fluid temperature, (F) 50°C fluid temperature, and (G) 60°C fluid temperature.

The achieved changes in surface wettability reveals the reduction in surface energy which can be linked to the physical chemistry phenomena of Hofmeister effect which suggests an increase in propensity of large ions toward hydrophobic surfaces [34]. These large ions tend to accumulate at the air/water interface causing an enhancement in surface hydrophobicity due to their weak interaction with the liquid compared with the liquid neighboring molecules interaction [35-37]. Table 2 summarises the testing parameters with their obtained contact angles.

Table 2. Testing parameters and obtained contact angles.

Temperature (^{o}C)	pH	Surface coating thickness (nm)	Average contact angle (degree)
10	4	0	78.62
10	4	50	80.15
10	4	100	83.94
10	4	150	91.13
10	7	0	75.7
10	7	50	70.72
10	7	100	70.51
10	7	150	68.42
10	9	0	77.02
10	9	50	82.23
10	9	100	86.39
10	9	150	90.1
20	4	0	74.34
20	4	50	92.06
20	4	100	92.25
20	4	150	97.83
20	7	0	72.2
20	7	50	70.04
20	7	100	69.46
20	7	150	67.94
20	9	0	78.46
20	9	50	87.97
20	9	100	92.07
20	9	150	94.99
25	4	0	70.92
25	4	50	78.69
25	4	100	81.47
25	4	150	92.07
25	7	0	70.19
25	7	50	69

25	7	100	58.15
25	7	150	55.26
25	9	0	70.35
25	9	50	74.57
25	9	100	77.3
25	9	150	85.72
30	4	0	83.97
30	4	50	86.4
30	4	100	89.97
30	4	150	95.36
30	7	0	74.13
30	7	50	71.6
30	7	100	67.05
30	7	150	65.51
30	9	0	80.27
30	9	50	84.72
30	9	100	87.88
30	9	150	92.12
40	4	0	73.82
40	4	50	81.05
40	4	100	91.92
40	4	150	93.43
40	7	0	73.35
40	7	50	72.54
40	7	100	70.34
40	7	150	69.85
40	9	0	77.67
40	9	50	88.75
40	9	100	92.6
40	9	150	96.19
50	4	0	79.16
50	4	50	86.78
50	4	100	88.8

50	4	150	93.98
50	7	0	77.4
50	7	50	72.81
50	7	100	70.67
50	7	150	68.54
50	9	0	82.69
50	9	50	88.9
50	9	100	91.34
50	9	150	97.03
60	4	0	70.25
60	4	50	80.3
60	4	100	90.94
60	4	150	94.55
60	7	0	68.42
60	7	50	65.71
60	7	100	61.17
60	7	150	56.25
60	9	0	71.02
60	9	50	78.49
60	9	100	92.48
60	9	150	100.13

4. Conclusion

Surface wettability experiments were conducted for a set of aluminium coated and uncoated substrates of aluminium origin at room temperature and DIW, of pH 4, 7, and 9, temperature ranging from 10°C up to 60°C. The elemental analysis were examined using X-ray fluorescent and x-ray diffraction analysers. From both analysers, it was conformed that the substrates used contained mostly aluminium, more than 90%, in their elemental structure.

The surface topography and liquid contact angle were also examined using an atomic force microscopy and a contact angle goniometer devices. From the atomic force microscopy tests, it was shown that the mean surface roughness was reduced by 60.46% to a value of 4.23 nm

after depositing 150 nm layer of aluminium particles on the substrate surface with the height range of the structures on the surface decreasing from 33.3 – 99.8 nm to 32.8 – 52.4 nm.

Contact angle studies on the substrates using DIW of pH 4, 7, and 9, at different liquid temperatures (i.e. 10°C to 60°C), showed changes in the surface behaviors which is believed to be influenced by the free ions hosted by the adjacent liquid and the contact surface as explained by the Hofmeister theory. Thus water with large free ions tends to reduce the surface energy and hence increasing the repellence level toward the liquid. This was concluded from previous researchers work [34-37] and our obtained data, as the contact angle of DIW showed a minimum CA value of 55.3° at a pH of 7, fluid temperature of 25°C, and film thickness of 150 nm. A maximum CA value of 100.1° was obtained when the DIW was adjected to a pH value of 9, fluid temperature of 60°C, and deposition thickness of 150 nm. In general, our results showed that water, of neutral charge, tends to form a higher hydrophilic relation with the surface. This attraction increases as the difference in surface structural heights decreases, and vice versa. It also suggest that hydrophilic surfaces tend to change their nature towards hydrophobicity when smoothen and coming in contact with water hosting free charges.

In conclusion, this article has focused on integrating particle deposition method with surface topography experiments and contact angle measurements for aluminium substrates with diverse DIW pH values and temperatures. It was shown that each of these techniques counterpart one another in providing an understanding towards the nature of activities occurring between the liquid and the surface in contact to it. In the future, it would be interesting to study and monitor the wettability behavior of aluminium/DIW nanofluids on nanocoated substrates. The impact of important parameters such as particle shape, volume percentage, fluid temperature, and sonication time on the hydrophobicity and hydrophilicity of the surface will be investigated. These experiments would be very useful into promoting the usage of nanofluids in industrial applications. This article represents the steps needed toward this direction.

Acknowledgements

This work was supported by the Kuwait Institute for Scientific Research (KISR). We acknowledge the help provided by Prof. M. Sherif El-Eskandarany, the program manager of Nanotechnology and Advanced Materials Program at KISR, for providing the required consumable materials used in this research. We also acknowledge and are grateful to Dr.

Sameera Al-Sayed Omar, KISR director general, for making the needed equipment's available and accessible throughout our conducted work.

References

[1] M.E. Burnett, S.Q. Wang, Current sunscreen controversies: a critical review, Photodermatology, photoimmunology & photomedicine, 27 (2011) 58-67.

[2] D. Lapotko, Erratum: Plasmonic nanoparticle-generated photothermal bubbles and their biomedical applications (Nanomedicine (Nanomedicine [Lond.]) (2009) 4:7 (813-845)), Nanomedicine, 11 (2009) 566.

[3] K. Maier-Hauff, R. Rothe, R. Scholz, U. Gneveckow, P. Wust, B. Thiesen, A. Feussner, A. Deimling, N. Waldoefner, R. Felix, A. Jordan, Intracranial thermotherapy using magnetic nanoparticles combined with external beam radiotherapy: Results of a feasibility study on patients with glioblastoma multiforme, J. Neuro-Oncol., 81 (2007) 53-60.

[4] B. Xu, Y. Qiao, Y. Li, Q. Zhou, X. Chen, An electroactuation system based on nanofluids, Appl. Phys. Lett., 98 (2011).

[5] J. Routbort, D. Singh, G. Chen, Heavy vehicle systems optimization merit review and peer evaluation, Annual Report, Argonne National Laboratory, Chicago, Illinois, USA, (2006).

[6] D.P. Kulkarni, D.K. Das, R.S. Vajjha, Application of nanofluids in heating buildings and reducing pollution, Appl. Energy, 86 (2009) 2566-2573.

[7] L. Vékás, D. Bica, M.V. Avdeev, Magnetic nanoparticles and concentrated magnetic nanofluids: Synthesis, properties and some applications, China Particuology, 5 (2007) 43-49.

[8] T. Sharma, A.L. Mohana Reddy, T.S. Chandra, S. Ramaprabhu, Development of carbon nanotubes and nanofluids based microbial fuel cell, Int J Hydrogen Energy, 33 (2008) 6749-6754.

[9] R. Taylor, S. Coulombe, T. Otanicar, P. Phelan, A. Gunawan, W. Lv, G. Rosengarten, R. Prasher, H. Tyagi, Small particles, big impacts: A review of the diverse applications of nanofluids, J. Appl. Phys., 113 (2013).

[10] Ş. Çolak, C. Aktürk, Synthesis and Characterization of Undoped and Doped (Mn, Cu, Co) ZnO Nanoparticles: An EPR Study, in: A.K. Shukla (Ed.) EMR/ESR/EPR Spectroscopy for Characterization of Nanomaterials, Springer India, New Delhi, 2017, pp. 151-179.

[11] R. Uyeda, Studies of ultrafine particles in Japan: Crystallography. Methods of preparation and technological applications, Prog Mater Sci, 35 (1991) 1-96.

[12] N. Ichinose, Y. Ozaki, S. Kashū, Applications of Superfine Particles, in: Superfine Particle Technology, Springer London, London, 1992, pp. 163-219.

[13] H. Gleiter, Nanostructured materials: basic concepts and microstructure, Acta Mater, 48 (2000) 1-29.

[14] A. Bertsch, S. Jiguet, P. Renaud, Microfabrication of ceramic components by microstereolithography, J Micromech Microengineering, 14 (2004) 197-203.

[15] J. Cho, M.S. Joshi, C.T. Sun, Effect of inclusion size on mechanical properties of polymeric composites with micro and nano particles, Compos. Sci. Technol., 66 (2006) 1941-1952.

[16] N. Vigneshwaran, P.V. Varadarajan, R.H. Balasubramanya, Application of Metallic Nanoparticles in Textiles, in: Nanotechnologies for the Life Sciences, Wiley-VCH Verlag GmbH & Co. KGaA, 2007.

[17] Y.C. Sharma, V. Srivastava, S.N. Upadhyay, C.H. Weng, Alumina nanoparticles for the removal of Ni(II) from aqueous solutions, Ind. Eng. Chem. Res., 47 (2008) 8095-8100.

[18] Y. Ding, H. Chen, Z. Musina, Y. Jin, T. Zhang, S. Witharana, W. Yang, Relationship between the thermal conductivity and shear viscosity of nanofluids, in: 3rd International Symposium on Functional Materials 2009, ISFM 2009, Jinju, 2010.

[19] R.B. Vignesh, J. Balaji, M.G. Sethuraman, Surface modification, characterization and corrosion protection of 1,3-diphenylthiourea doped sol-gel coating on aluminium, Prog Org Coatings, 111 (2017) 112-123.

[20] L. Jodin, A.C. Dupuis, E. Rouvière, P. Reiss, Influence of the catalyst type on the growth of carbon nanotubes via methane chemical vapor deposition, J Phys Chem B, 110 (2006) 7328-7333.

[21] W. Cai, J. Yu, B. Cheng, B.L. Su, M. Jaroniec, Synthesis of boehmite hollow core/shell and hollow microspheres via sodium tartrate-mediated phase transformation and their enhanced adsorption performance in water treatment, J. Phys. Chem. C, 113 (2009) 14739-14746.

[22] X. Yu, J. Yu, B. Cheng, M. Jaroniec, Synthesis of hierarchical flower-like AlOOH and TiO 2/AlOOH superstructures and their enhanced photocatalytic properties, J. Phys. Chem. C, 113 (2009) 17527-17535.

[23] M. Najafzadeh, J. Shiri, G. Sadeghi, A. Ghaemi, Prediction of the friction factor in pipes using model tree, ISH Journal of Hydraulic Engineering, (2017) 1-7.

[24] M. Kang, J.W. Lee, Y.T. Kang, Reduction of liquid pumping power by nanoscale surface coating, International Journal of Refrigeration, 71 (2016) 8-17.

[25] S.P. Rodrigues, C.F.A. Alves, A. Cavaleiro, S. Carvalho, Water and oil wettability of anodized 6016 aluminum alloy surface, Applied Surface Science, 422 (2017) 430-442.

[26] Z. Ahmad, EFFECT OF VELOCITY ON THE OPEN CIRCUIT POTENTIAL AND CORROSION RATE OF ALUMINIUM ALLOYS, Met Corros Ind, 60 (1985) 289-296.

[27] Z. Ahmad, The kinetics of anodic and cathodic polarization of aluminium and its alloys, Anti-Corros. Methods Mater., 33 (1986) 4-11.

[28] X. Tian, Y. Li, S. Wan, Z. Wu, Z. Wang, Functional Surface Coating on Cellulosic Flexible Substrates with Improved Water-Resistant and Antimicrobial Properties by Use of ZnO Nanoparticles, J. Nanomater., 2017 (2017).

[29] E.B. Caldona, A.C.C. de Leon, B.B. Pajarito, R.C. Advincula, Novel anti-corrosion coatings from rubber-modified polybenzoxazine-based polyaniline composites, Applied Surface Science, 422 (2017) 162-171.

[30] X. Zhang, Y. Wang, D. Zhao, J. Guo, Improved thermal performance of heat exchanger with TiO2 nanoparticles coated on the surfaces, Appl Therm Eng, 112 (2017) 1153-1162.

[31] H.T. Phan, N. Caney, P. Marty, S. Colasson, J. Gavillet, Surface wettability control by nanocoating: The effects on pool boiling heat transfer and nucleation mechanism, Int. J. Heat Mass Transf., 52 (2009) 5459-5471.

[32] E. Akbari, A.M. Gheitaghy, H. Saffari, S.M. Hosseinalipour, Effect of silver nanoparticle deposition in re-entrant inclined minichannel on bubble dynamics for pool boiling enhancement, Exp. Therm. Fluid Sci., 82 (2017) 390-401.

[33] S. Hariprasad, S. Gowtham, S. Arun, M. Ashok, N. Rameshbabu, Fabrication of duplex coatings on biodegradable AZ31 magnesium alloy by integrating cerium conversion (CC) and plasma electrolytic oxidation (PEO) processes, J Alloys Compd, 722 (2017) 698-715.

[34] U. Sivan, The inevitable accumulation of large ions and neutral molecules near hydrophobic surfaces and small ions near hydrophilic ones, Curr. Opin. Colloid Interface Sci., 22 (2016) 1-7.

[35] J. Morag, M. Dishon, U. Sivan, The governing role of surface hydration in ion specific adsorption to silica: An AFM-based account of the hofmeister universality and its reversal, Langmuir, 29 (2013) 6317-6322.

[36] I. Schlesinger, U. Sivan, New Information on the Hydrophobic Interaction Revealed by Frequency Modulation AFM, Langmuir, 33 (2017) 2485-2496.

[37] N. Schwierz, D. Horinek, U. Sivan, R.R. Netz, Reversed Hofmeister series—The rule rather than the exception, Curr. Opin. Colloid Interface Sci., 23 (2016) 10-18.

Highlights

- An approach used in modifying surface wettability is proposed.
- The mechanism relies on the famous Hofmeister theory of ionic interaction.
- Particle deposition and fluid pH level are the key elements of this approach.

2018-02-27

The effect of aluminium nanocoating and water pH value on the wettability behavior of an aluminium surface

Ali, Naser

Elsevier

Naser Ali, Joao A. Teixeira, Abdulmajid Addali, et al., The effect of aluminium nanocoating and water pH value on the wettability behavior of an aluminium surface. Applied Surface Science, Volume 443, 15 June 2018, Pages 24-30

https://doi.org/10.1016/j.apsusc.2018.02.182